Joint International IMEKO TC1+ TC7+ TC13 Symposium
August 31st – September 2nd, 2011, Jena, Germany
urn:nbn:de:gbv:ilm1-2011imeko:2

A COMPACT SMART RESISTIVE SENSOR BASED ON A MICROCONTROLLER

Zbigniew Czaja

Faculty of Electronics, Telecommunications and Informatics, Gdansk University of Technology, Gdansk, Poland

Abstract – A new solution of the smart resistance sensor basing on a microcontroller, for which the resistance sensor is a component of an anti-aliasing filter of an ADC is proposed. The temperature measurement procedure bases on stimulation of the filter by square impulses and on sampling the time response of the filter, and next on decoding the measurement voltage result to the temperature value. All steps of the measurement procedure are realized by the microcontroller and its internal devices (timers and an ADC).

Keywords: microcontrollers, smart resistive sensors

1. INTRODUCTION

Nowadays, more and more sensors are produced as smart sensors in one chip controlled via digital interfaces (SPI, I^2C or 1-Wire). But, e.g. many temperature sensors cannot be made in this technology, what follows from the limited range of operating temperature of the chip. Hence, resistance sensors (e.g. the Pt100) or thermocouples are still used.

In typical measurement applications of resistance sensors, the resistance is measured based on resistance bridges and high resolution Σ-Δ ADCs [1] or based on circuits in which the sensor is stimulated by a DC current source and the voltage on the sensor is amplified, filtered and next measured by an ADC [2]. These applications are complex and they are not very suitable for simple measurement systems with a battery power supply often working as endpoints in sensor wireless networks (e.g. based on the ZigBee protocol).

Obviously, there are solutions for which resistive sensors [3,4], differential resistive sensors [5] and resistive sensors bridges [6,7] are directly connected to a microcontroller without any intermediate active components. Such a direct interface circuit relies on measuring the discharging time of a *RC* network that includes the resistances of the sensor. But, in these cases the resistance measurement is burdened with big uncertainly, which follows from parameters of the microcontroller pin and influence of disturbances, because the measurement circuit is not equipped with an anti-aliasing filter.

Therefore, a new measurement interface basing on the microcontroller for resistance sensors is proposed in the paper. This interface together with the sensor forms a compact smart resistance sensor.

2. THE SMART RESISTANCE SENSOR

2.1. The architecture of the sensor

The proposed smart sensor is a very simple measurement system for resistance sensors (Fig. 1). The main idea of this approach is the fact that the sensor is part of the anti-aliasing filter of the ADC.

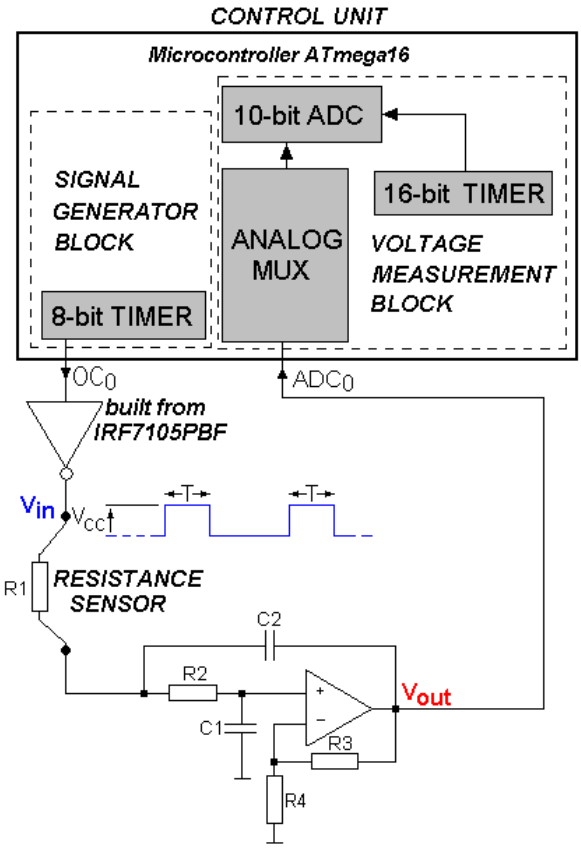

Fig. 1. A compact smart resistance sensor controlled by the microcontroller

The microcontroller controls the whole measurement system. Its internal 8-bit timer controls the duration time of two square impulses which stimulate the 2nd-order low band-pass Sallen-Key filter with the gain equal to 3 (Fig. 1). The stimulation signal is generated on the OC0 pin. It passes through the inverter built from an IRF7105PBF (Fig. 2). In this way we eliminate the influence of electrical parameters (espe-

cially the output pin variable impedance) of the OC0 output pin on the stimulation signal. The IRF7105 consists of two HEXFET power MOSFETs, the first one with a N-channel and the second one with a P-channel [8]. Additionally, it has small values of static drain-to-source on-resistances (0.1 Ω and 0.25 Ω for N-channel and P-channel transistors respectively) and big values of continuous drain currents (3.5 A and –2.3 A adequately).

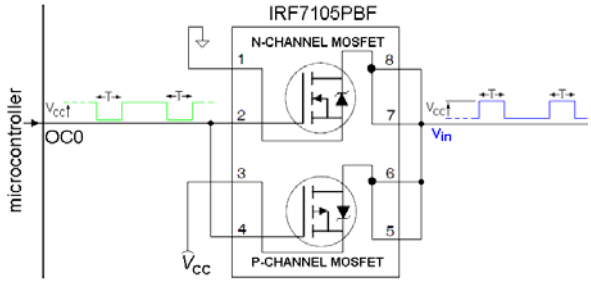

Fig. 2. The inverter basing on the IRF7105 introduced between the OC0 output of the microcontroller and the sensor

As an example of the resistance sensor the Pt100 sensor is used, marked as R_1. Hence, nominal values of the ant-aliasing filter are the following: R_1 (Pt100) = 110 Ω, R_2 = 110 Ω, R_3 = 20 kΩ, R_4 = 10 Ω, C_1 = 1,022 μF, C_2 = 2,038 μF. It is assumed that the nominal value of R_1 is equal to 110 Ω, what corresponds to about 26°C (according to PN-EN 60751+A2), and its values change from 0.2 to 4 ? of its nominal value (what corresponds to temperatures from about –192 °C to 850 °C).

2.2. The measurement procedure

The temperature measurement procedure consists of a measurement step in which the filter with the sensor is stimulated and two voltage values V_1 and V_2 of the time response are measured, and a determination step in which the temperature is determined basing on these results.

As shown in Fig. 3, the time response of the ant-aliasing filter for the first square impulse is sampled by the internal 10-bit ADC at moment t_1 (the V_1 sample) and the second one at moment t_2 (the V_2 sample) established by the 16-bit timer.

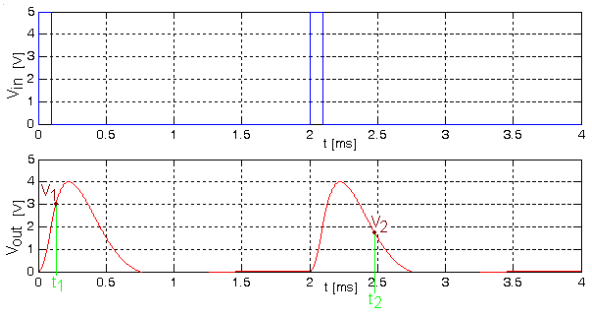

Fig. 3. Square stimulation impulses and time responses of the 2nd-order low band-pass Sallen-Key filter (with the gain equal to 3) at its output

The samples V_1 and V_2 are treated as coordinates of the measurement point. Hence, temperature determination bases on placing this point into the measurement space with the identification curve of component R_1 (Pt100) scaled with the temperature values (Fig. 4). That is, the position of this point on the curve directly points to the temperature value.

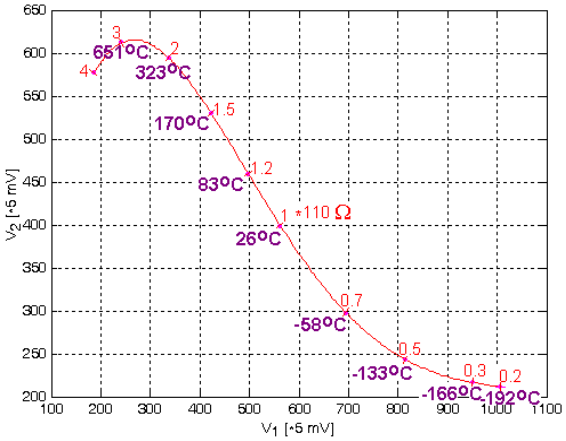

Fig. 4. The identification curve of component R_1 (Pt100) in the measurement space scaled in temperature values

The curve is a graphical illustration of the dictionary containing the conversion table consisting of the following set: $\{(V_1^j, V_2^j) \rightarrow T^j\}_{j=1,2,...,J}$, where J is the number of discrete values of temperature in the assumed range of its changes. The curve was generated in the pre-testing stage according to the rules described in [9,10]. Hence, it illustrates the behaviour of the filter following from changes of R_1 component values. The range of resistance value changes was set and the curve scaling in the temperature values was made according to PN-EN 60751+A2. This solution allows to simplify calculations made by the microcontroller.

2.3. Assignment of parameters of the stimulation signal and response signal

Location and shape of the curve, that is its optimal scaling allowing to permit the best reading of the temperature, exclusively depend on the duration time of the impulses t_d, the number of the impulses K, moments t_1, t_2 … t_K of voltage samples of the response signal, and the gain A of the filter. So it is very important to determine these parameters.

The duration time of the square impulse is assigned in two steps in the same way as described in [9]. In the first step, this time is set to a value $t_d = 1/f_c$, where f_c is the cut-off frequency of the filter. In the second step we fix the maximum value of the output signal $V_{out}=\xi \cdot V_{in}$ for nominal values of elements of the circuit, where coefficient $\xi \in < 0, 1 >$. Next we fit the duration time t_d in a simulated way to obtain a given maximum value V_{out} of the output signal.

It is known [11] that the number K of measured parameters of the filter needed for correct value identi-

fication of one component, that is the size of the measurement space K, should be at least equal to 2.

Obviously, an increase of the number K leads to an improvement of the identification resolution. It follows from the fact that enlargement of the size of the measurement space implies increasing the distances between scale points of the identification curve [12]. An increase of the identification resolution is more effective for small K, because as proved in [10]: if $K \to \infty$, $t_{k+1} - t_k \to 0$ and $V_{k+1} - V_k \to 0$. We also should remember that the size of the dictionary linearly depends on K.

Taking the above considerations into account the number K should not be big, e.g. $K = 2, .., 4$ is suggested. This number is obviously dependent on the topology of the chosen filter. It should be small, but enabling the reading of the temperature with the required resolution.

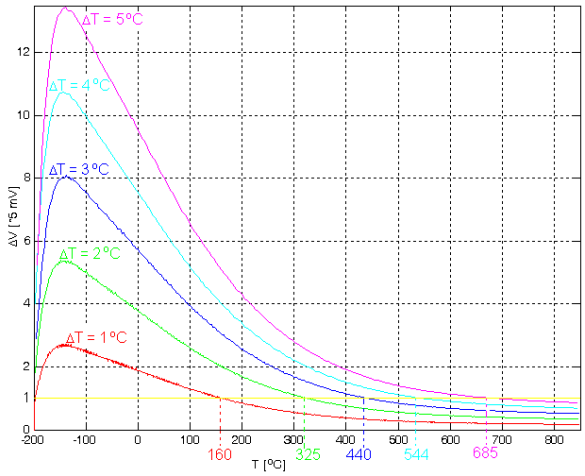

Fig. 5. Charts of voltage measurement resolution for a 10-bit ADC of the microcontroller for given temperature resolutions and for $K = 2$ in function of the measurement temperature

Fig. 5 shows the charts of voltage measurement resolution for a 10-bit ADC of the microcontroller for given temperature resolutions and for $K = 2$ in function of the measurement temperature. It is seen that for the 10-bit resolution of voltage measurement we can determine temperature ranges with given temperature reading resolution ΔT. It follows from the fact that there are temperatures for which a change of the resistance value of the Pt100 following from the change of the temperature values with a given ΔT step gives the change of the V_1 and V_2 values below the 10-bit ADC resolution (less than 1 LSB).

Similar investigations were made for the 10-bit ADC and $K = 3$ and also for the 12-bit ADC ($K = 2$, $K = 3$). All results are collected in Table 1. It is seen that increasing the number K extends the temperature range for the given temperature resolution. However, if it is required, to measure with possibly the best temperature resolution in possibly the largest temperature range, we should use the external 12-bit ADC connected to the microcontroller. But, we should remember that this improvement considerably increases the costs.

TABLE I. Temperature ranges for assumed temperature resolution measurement for 10-bit and 12-bit ADCs (where: "full range" - -200 : 850)

ΔT [°C]	10-bit ADC temp. range [°C]		12-bit ADC temp. range [°C]	
	$K = 2$	$K = 3$	$K = 2$	$K = 3$
1	-200 : 160	-200 : 246	-200 : 535	-200 : 708
2	-200 : 325	-200 : 458	full range	full range
3	-200 : 440	-200 : 597	full range	full range
4	-200 : 544	-200 :706	full range	full range
5	-200 : 685	-200 :815	full range	full range

The way of determination of moments of voltage samples depends on the number K of voltage samples. Hence, it is different e.g. for $K = 2$ and for $K = 3$.

For $K = 2$ two moments t_1 and t_2 are determined based on criteria of the best identification resolution. It is similar to the criteria presented in [9]. Hence, the moment t_1 is determined in the first step $t_1 \in (0, t_d)$ – during the duration of the stimulation impulse, and the moment t_2 in the second one $t_2 \in (t_d, t_p)$, – in the time between subsequent impulses.

To determine these moments, a coefficient λ was introduced. It describes the difference between the maximum and minimum values of the voltage of the filter responses at moment t_n for a defined range of changes of values of the R_1 component:

$$\lambda(t_n) = \max_{j=1,..,J} \{u(R_{1j}, t_n)\} - \min_{j=1,..,J} \{u(R_{1j}, t_n)\}. \qquad (1)$$

where J – the number of values of the R_1 component in the range from 0.2 to 4 of its nominal value.

Thus we can define:

$$\lambda_{\max 1} = \max_{n=1,..,N_1,\ t_k \in (0, t_d)} \{\lambda(t_n)\} \qquad (2a)$$

and

$$\lambda_{\max 2} = \max_{n=N_1,..,N_2,\ t_k \in (t_d, t_p)} \{\lambda(t_n)\} \qquad (2b)$$

where N_1, N_2, – the number of samples for the time range $(0, t_d)$ and $(0, t_p)$ respectively.

Hence, the solutions of (2) determine the two moments of voltage samples:

$$\lambda_{\max 1} \to t_1 \quad \text{and} \quad \lambda_{\max 2} \to t_2 \qquad (3)$$

For the filter from Fig. 1 the following moments of voltage samples $t_1 = 120$ µs and $t_2 = 460$ µs were determined. For these moments, the identification curve of the R_1 component on the plane V_1, V_2 is drawn in Fig. 4, and also in Fig. 6.

The last parameter which has to be determined, is the gain A of the filter. The gain A should be on the level allowing the use of the full measurement range of the ADC, but for the full assumed temperature

measurement range the values of V_1 and V_2 should not exceed the range value of the ADC (1024 LSB).

The identification curves for the R_1 component for different A values are shown in Fig. 6.

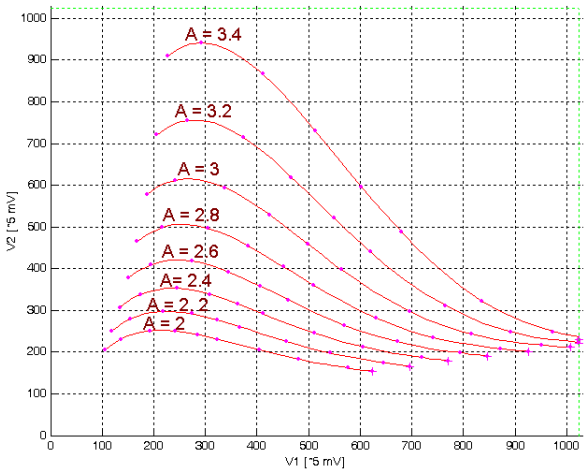

Fig. 6. Identification curves of R_1 component (Pt100) in the measurement space for different values of the gain A

It is seen that the best fitting of the identification curve to the measurement space is for $A = 3$. For bigger values of A, V_1 exceeds 1024 LSB, and for smaller ones the curves are so short, that is they characterize a too small temperature scale.

3. CONCLUSION

A new solution of the smart resistance sensor basing on the microcontroller, for which the resistance sensor is a component of the anti-aliasing filter of the ADC is proposed. The architecture of the smart sensor, the temperature measurement procedure and determination of the sensor system parameters are included in the paper. The proposed smart resistance sensor has the following advantages:

- The circuit of the sensor is small and very simple what decreases costs and reduces the size of the system.
- Stimulation signals are generated and measurements are made only by internal devices of the microcontroller, which also can serve the function of a wireless communication controller.
- For temperature measurement with 1°C resolution the 12-bit ADC, and even the 10-bit ADC is sufficient (obviously, for a narrower temperature measurement range) what follows from e.g. multiple measurements made during the measurement procedure.
- The duration time of the temperature measurement procedure is short. Hence, the system can be activated only during this procedure, it can be in a sleep mode in the remaining time, what reduces the power consumption. Thanks to this, this solution is ideal for battery-power-supplied systems.

REFERENCES

[1] C. Eckert, R. Bax, *Practical RTD Interface*, National Semiconductor Corporation, Application Note 1559, June 2007.

[2] M. Leinonen, J. Juuti, H. Jantunen, "Interface circuit for resistive sensors utilizing digital potentiometers", *Sensors and Actuators A*, vol. 138, issue 1, pp. 97–104, July 2007.

[3] F. Reverter, M. Gasulla, R. Pallàs-Areny, "Analysis of Power-Supply Interference Effects on Direct Sensor-to-Microcontroller Interfaces", *IEEE Transactions on Instrumentation and Measurement*, vol. 56 no. 1, pp. 171-177, February 2007.

[4] F. Reverter, J. Jordana, M. Gasulla, R. Pallàs-Areny, "Accuracy and resolution of direct resistive sensor-to-microcontroller interfaces, *Sensors and Actuators A*, vol. 121, issue 1, pp. 78–87, May 2005..

[5] F. Reverter and O. Casas, "Interfacing Differential Resistive Sensors to Microcontrollers: A Direct Approach", *IEEE Transactions on Instrumentation and Measurement*, vol. 58 no. 10, pp. 3405-3410, October 2009..

[6] E. Sifuentesa, O. Casasa, F. Reverter, R. Pallàs-Areny, "Direct interface circuit to linearise resistive sensor bridges", *Sensors and Actuators A*, vol. 147, issue 1, pp. 210-215, September 2008..

[7] J. Jordana, R. Pallàs-Areny, "A simple, efficient interface circuit for piezoresistive pressure sensors", *Sensors and Actuators A*, vol. 127, issue 1, pp. 69-73, February 2006..

[8] International Rectifier, IRF7105 HEXFET Power MOSFET, PDF file, (2003)

[9] Z. Czaja, "A diagnosis method of analog parts of mixed-signal systems controlled by microcontrollers", *Measurement*, vol. 40, issue 2, pp. 158-170, February 2007.

[10] Z. Czaja, "A method of fault diagnosis of analog parts of electronic embedded systems with tolerances", *Measurement*, vol. 42, issue 6, pp. 903-915, July 2009.

[11] Liu R.: Testing and diagnosis of analog circuits and systems, Van Nostrand Reinhold, USA, New York, 1991.

[12] Z. Czaja, R. Zielonko, "On fault diagnosis of analogue electronic circuits based on transformations in multi-dimensional spaces", *Measurement* vol. 35, issue 3, pp. 293-301 , April 2004.

Author: dr. eng. Zbigniew Czaja, Department of Optoelectronics and Electronic Systems, Faculty of Electronics, Telecommunications and Informatics, Gdansk University of Technology, ul. G. Narutowicza 11/12, 80-233 Gdansk, Poland, phone 48 58 347-14-87, fax. 48 58 347-13-57, zbczaja@pg.gda.pl.